Geolocation of AMSR-E data

Heidrun Wiebe, Georg Heygster, and Lothar Meyer-Lerbs
Institute of Environmental Physics, University Bremen, 28334 Bremen, Germany
Tel.:+49-421-218-4274, Fax:+49-421-218-4555, Email:hwiebe@uni-bremen.de

***Abstract*—The process of determining the geographic latitude and longitude (short: lat/lon) of the center point of the footprint is called geolocation, which is currently suboptimal for AMSR-E (Advanced Microwave Scanning Radiometer for Earth Observing System) Level 1 data provided by the Japan Aerospace Exploration Agency (JAXA). Here we present a study for improving the geolocation. The viewing angles (nadir angle and scan angle) that define the boresight direction of the instrument are optimized and new lat/lon coordinates are calculated. The optimization method is based on minimizing differences between ascending and descending swaths.**

The results of the here calculated viewing angles have an overall standard deviation of 0.005°, which is 170 m on ground for the nadir angle and 70 m for the scan angle. The residual geolocation error ranges between 425 m (89 GHz) and 1425 m (6 GHz). The averaged repositioning between JAXA and our geolocation ranges between 3.5 km and 7 km, i.e. in the order of one footprint size at 89 GHz. A comparison with a similar study, performed by Wentz, shows good agreement in the viewing angles, the RMS of the differences is 0.0083° ($\approx$ 283 m) for the nadir angle and 0.0132° ($\approx$ 191 m) for the scan angle.

I. INTRODUCTION

Retrieval of surface and atmospheric parameters from passive microwave sensors in most cases requires simultaneous use of data taken at different frequencies, and that all involved channels represent the correct location of the Earth's surface or atmosphere. As the data are typically taken by different feedhorns and the same antenna reflector, they may point to different regions on the Earth, in addition they may have different resolutions. As a first step to co-locate the data of different frequencies in near real time, the exact position of the data on the Earth, called geolocation, needs to be determined.

This paper presents a geolocation study of the data of the passive microwave sensor AMSR-E (Advanced Microwave Scanning Radiometer for Earth Observing System) developed by the Japan Aerospace Exploration Agency (JAXA). It operates on the satellite Aqua launched in May 2002. It observes at seven frequencies ranging from 6 GHz to 89 GHz, each one measuring at horizontal and vertical polarization. Detailed description of the AMSR-E instrument is given in [4], [1], and [2]. The geolocation of AMSR-E Level 1 data is currently not optimal, which can in particular be seen along coastlines due to the high land–sea contrast in brightness temperatures (Figure 3, detailed discussion see Section III-A).

Further observations of the geolocation error show that the projected footprints are shifted in the satellite flight direction. That means footprints of ascending swaths are shifted towards north-west, those of descending swaths towards south-west. Consequently, the brightness temperature differences between ascending and descending swaths of one day are expected to be quite high along coastlines. The top image of Figure 4 (detailed discussion see Section III-A) shows those differences at 89 GHz (map of Scandinavia and Baltic States), where we have positive differences (yellow and red colors) along north coasts, and negative differences (blue and violet colors) along south coasts. This observation leads to the approach for optimizing the geolocation: the lower the absolute values of the differences, the better the geolocation.

The goal of the work presented here is to retrieve parameters for the viewing angles of the satellite instrument with which a more accurate projection of measured brightness temperatures to latitude and longitude (short: lat/lon) coordinates can be achieved. The method to improve the geolocation of AMSR-E data is to determine optimal constant offsets for all nadir and scan angles of the measurements given in the AMSR-E Level 1 data. Based on these values, the lat/lon boresight coordinates for each footprint are recalculated. This method is similar to a previous geolocation study [6]. However, here we will restrict the analysis to near-coast pixels.

II. GEOLOCATION OPTIMIZATION

The approach of improving the geolocation of AMSR-E data is finding the boresight direction by minimizing the absolute brightness temperature differences between ascending and descending swaths. The boresight direction is determined by the orientation of the satellite and the offsets for the viewing angles (nadir angle and scan angle, Figure 1) of the AMSR-E instrument.

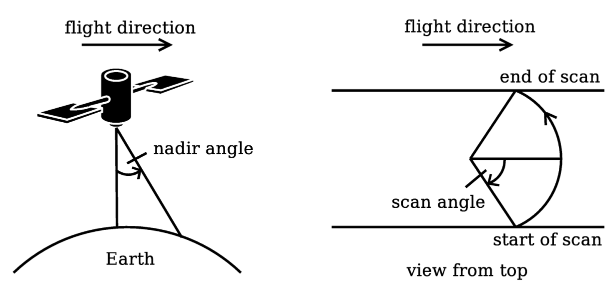

Fig. 1. Viewing geometry of the AMSR-E instrument

The nadir angle is the angle between nadir and boresight direction. The scan angle is the angle between right swath edge and swath center of the conically scanning antenna, measured on the cone-shaped shell.

The parameters that define the orientation of the satellite are rotations in three dimensions around the satellite's coordinate system origin, the center of mass (Figure 2). Roll gives the rotation around the x-axis (flight direction), pitch around the y-axis and yaw around the z-axis. The values for roll, pitch and yaw angle (given in the AMSR-E data set) are very accurate as the geolocation of MODIS (Moderate Resolution Imaging Spectroradiometer, operating on the same platform as AMSR-E) is precise up to the resolution of MODIS, i.e. 250 m ([8], [9]). Therefore, the angles that need to be adjusted are only the AMSR-E specific angles: nadir and scan angle. The roll angle offset relative to the spacecraft frame is set to 0.09°, as it is given in [6]. By varying this offset in steps of 0.005° and using the optimized nadir and scan angles, the roll angle offset was confirmed. A detailed description of the projection routine is given in [5].

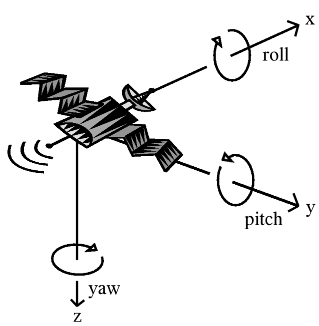

Fig. 2. Orientation of the satellite: roll, yaw and pitch, flight direction is along x-axis

The acquisition of optimal values for the nadir angle and the scan angle is based on finding the minimum of absolute brightness temperature differences between maps of ascending and descending swaths of one day. Thus, the values of the viewing angles have to be varied until the minimum is reached. In order to focus the difference data on the geolocation error, the analysis is restricted to data along coastlines. The coastline stripe is obtained by using built-in functions of the geographic mapping tool GMT, which uses the World Vector Shoreline (WVS)[1] for the destinction between saltwater and land: all sea pixels are set to 0, all land pixels to 1, from the resulting image the gradient is taken. Consequently, all pixels that are not 0 are selected to be coastline pixels and set to 1. Finally, each pixel of the difference image (containing the brightness temperature differences of ascending minus descending swaths) is multiplied with each pixel of the coastline image. The width of the coastline stripe is around 20 km.

The geolocation method is applied to data of 16 days (the first day of each quarter year from January 2003 to October 2006) using global coverage. The averages of those 16 days are taken as the global optimal viewing angles. As the feedhorns for the different frequencies of the AMSR-E instrument are looking in slightly different directions, the geolocation method is applied to all AMSR-E feedhorns, each one corresponding to a frequency band.

[1] URL http://www.csc.noaa.gov/shoreline/world_vec.html

III. Geolocation Results

The results obtained by applying the geolocation optimization method, henceforth called IUP (Institute of Environmental Physics, University Bremen) geolocation, are analyzed visually and numerically. First, the JAXA geolocation is compared to the IUP geolocation in Sections III-A and III-B. The numerical analysis (Section III-C) deals with the viewing angles, their standard deviation and their time series analysis. Finally, the results are compared to those obtained by Wentz [6] in Section III-D.

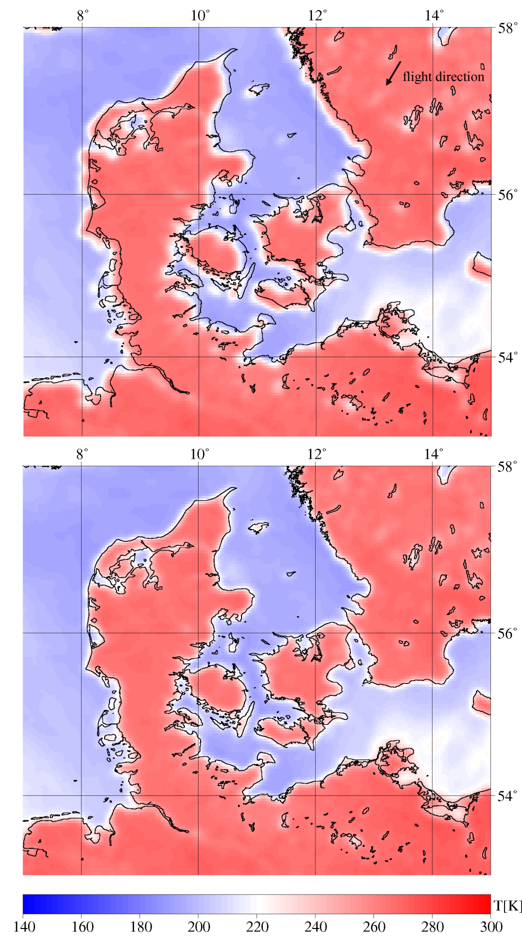

Fig. 3. Brightness temperatures of Channel 89 GHz B-scan H-pol. (map of Denmark), October 01, 2004, top: JAXA geolocation, bottom: IUP geolocation

A. Visual Analysis of Geolocation

The visual analysis of brightness temperature images before and after adjusting the viewing angles shows a considerable improvement in the geolocation of the data. Figure 3 shows the brightness temperatures at 89 GHz over Denmark before (top image) and after (bottom image) adjustment. The maps are produced with the geographical mapping tool GMT by interpolating footprints and overlaying coastlines. In the JAXA image some areas that correspond to land (reddish color) are located on water (seas and lakes), and some areas that refer to water (bluish color) are placed on land. In the IUP image in contrast, the geolocation is much more accurate, that means all reddish areas are on land and all bluish areas on water.

Looking at the brightness temperature differences between ascending and descending swaths, the improvements in geolocation can be demonstrated even more impressively. Figure 4 shows the differences of JAXA geolocation (top image) and those of IUP geolocation (bottom image). In the JAXA image there are large differences along coastlines, in the IUP image they are almost gone. In Table I, the numerical values of mean differences per pixel for one of the 16 days are given, which is representative for all other days. The mean differences per pixel are between 8.75 K and 15.74 K for JAXA geolocation, and between 4.94 K and 7.87 K for IUP geolocation. That means the mean differences have been reduced by factors between 1.6 and 2.7. However, differences may not only be caused by the geolocation error, but also from different surface temperatures at the acquisition time of ascending and descending overpasses (which typically are several hours apart), and from different atmospheric influences, i.e. weather effects. The latter mainly occurs in the higher frequency channels which are sensitive towards clouds.

TABLE I
MEAN DIFFERENCES PER PIXEL AT ALL AMSR-E FREQUENCIES FOR OCTOBER 01, 2004, RATIO = JAXA DIVIDED BY IUP

Channel	JAXA [K]	IUP [K]	Ratio
6 GHz	8.75	4.94	1.8
10 GHz	9.52	4.94	1.9
18 GHz	15.13	5.67	2.7
23 GHz	12.50	5.38	2.3
36 GHz	15.74	6.53	2.4
89 GHz A	12.23	7.87	1.6
89 GHz B	12.55	7.81	1.6

The residual error of the here calculated geolocation is shown in Figure 5. It ranges from 245 m for the 89 GHz channels to 1425 m for the 6 GHz channel. This corresponds to 5% of the footprint size for 89 GHz and between 2% to 3% for the lower frequencies. The method to obtain the residual geolocation error consists of calculating the cross correlation between two images with a 8-bit quantization. The reference image contains the land–ocean contrast where all ocean pixels are set to 0 and all land pixels to 255 generated from GMT's coastline data. The second image contains brightness temperatures (using our geolocation) scaled from 0 (lowest T_B value) to 255 (highest T_B value). From the cross correlation matrix the shift between the two images is calculated. The method is applied to the 16 selected days for the Northern Europe region shown in Figure 3, which is representative, as it contains many coastlines. Both images consist of 5664 by 4960 pixels for the 89 GHz channels and 2832 by 2480 pixels for the lower frequency channels; the area is 557 km by 505 km. The avarage and standard deviation over these 16 cross correlations give an estimate of the residual geolocation error for each channel. There was not trend in time observed (figures not shown here).

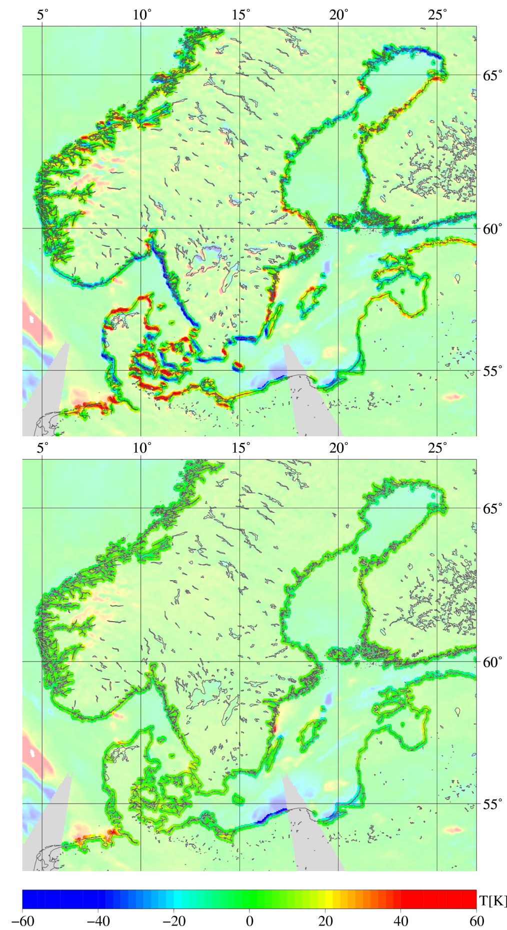

Fig. 4. Brightness temperature differences (ascending – descending) of Channel 89 GHz B-scan H-pol. (map of Scandinavia and Baltic States), October 01, 2004, top: JAXA geolocation, bottom: IUP geolocation

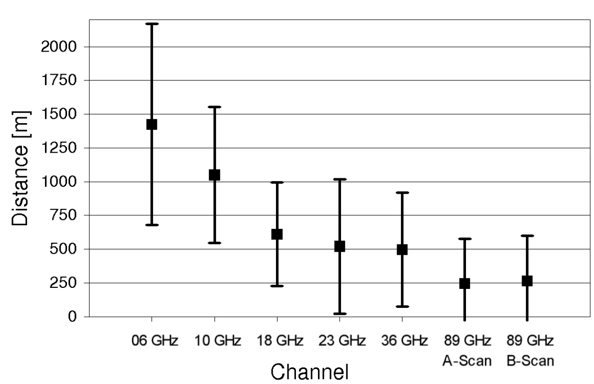

Fig. 5. Residual geolocation error calculated over the 16 selected days. No trend in time was observed.

B. Repositioning: JAXA – IUP

The repositioning between JAXA and IUP geolocation, i.e. the horizontal shift between those data, is shown for October 01, 2004 in Figure 6 (using the coregistration parameters for the lower frequency channels of the JAXA geolocation [2]). As the geolocation of our method is stable in time (Section III-A), we can take it as a reference. Averaged over all channels, the mean distances are 6.5 ± 1.9 km.

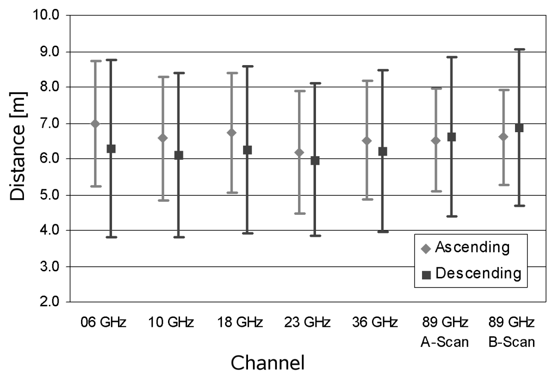

Fig. 6. Repositioning between JAXA and IUP geolocation for all swaths of October 01, 2004.

Investigating in more detail the mean distances for each of the channels reveals two things: First, the mean distances at the 89 GHz channels are higher for descending than for ascending swaths. In the lower frequency channels (6 GHz to 36 GHz) it is vice versa. This is assumed to be due to the JAXA co-registration function [2]. In the JAXA data only the lat/lon coordinates for the 89 GHz channels are given. The coordinates for the lower frequency channels are calculated by the JAXA co-registration function using the 89 GHz coordinates and two constant co-registration parameters for each frequency channel. As we have differences of mean distances between ascending and descending swaths in the 89 GHz channels, we also get differences in the lower frequency channels. As a result of the co-registration calculations, the mean distances at the lower frequency channels then get lower for descending swaths than for ascending ones. Thus, we would not expect this effect when the mean distances were equal for ascending and descending swaths. Second, the errors for descending swaths are higher (± 2.2 km) than for ascending ones (± 1.3 km). The left images of Figure 7 show the repositioning for one ascending (upper left image) and one descending (lower left image) swath of October 01, 2004. These are representative for all examined swaths at all AMSR-E channels. In general, the JAXA-IUP distances are less pronounced at the left side (relative to the flight direction) of the swaths, especially at higher latitudes. Descending swaths have, in contrast to ascending swaths, distances up to 12 km between $30°$ and $-30°$ latitude.

This asymmetry is in agreement with the analysis of the geolocation error by JAXA itself [3]. The results JAXA presented in 2005 state that the error depends on scan position

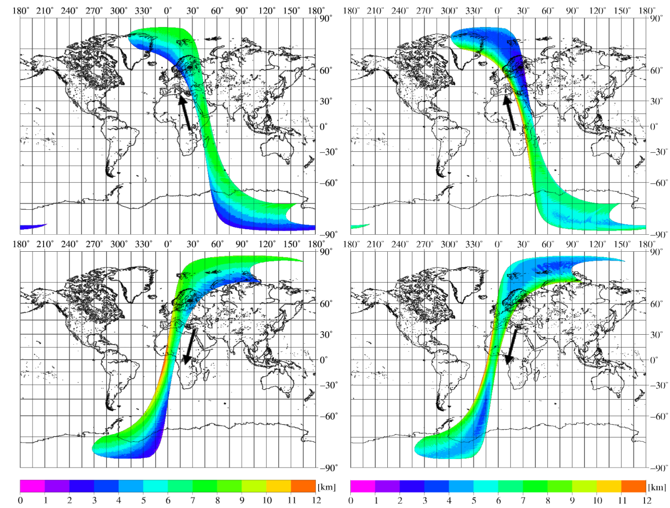

Fig. 7. Ascending (top images) and descending (bottom images) swaths of repositioning between JAXA and IUP geolocation, Channel 89 GHz B-scan H-pol., left images: October 01, 2004 (geolocation version 1), right images: October 01, 2006 (geolocation version 2). Black arrows indicate flight direction.

and is more pronounced in the descending swaths. Based upon this finding, JAXA developed a correction function, which is applied to the data in the geolocation of version 2 (released March 01, 2005). As the left images of Figure 7 originate from 2004, the JAXA correction is not applied. The mean distances over all swathes of that day are 6.6 ± 1.3 km for ascending, and 6.9 ± 2.2 km for descending swaths. That means the standard error is higher for descending swaths. The right images of Figure 7 originate from 2006, so the geolocation is adjusted by the JAXA correction function. We see that the distances are similar in the ascending (upper right image) and descending (lower right image) swath, but not the errors in distances of the descending swath did improve, the errors in distances of the ascending swath got even worse. The mean distances over all swaths of that day are 6.6 ± 2.1 km for ascending, and 6.7 ± 1.9 km for descending swaths. That means the standard error is similar for ascending and descending swaths with the correction function, whereas it increases from 1.3 km (without JAXA correction) to 2.1 km (with JAXA correction). However, there are still quite high mean distances of 6.65 km even with applying the correction function.

Examinations of repositioning changes with time reveal that the mean JAXA geolocation error of the 89 GHz channel follows a seasonal cycle (lowest in January/April, highest in October) overlayed by a rising trend (Figure 8). This holds for both the geolocation of version 1 and the one of version 2, whereas the error drops between the versions by about 2 km. As the coordinates of the lower frequency channels are calculated based on those of the 89 GHz channel, a similar trend is expected here. In general the error depends on scan position, but it is not associated with specific geographical regions, however it is more pronounced between $30°$ and $-30°$ latitude. The variation across the scan is high, it ranges between 2 km and 12 km (Figure 7).

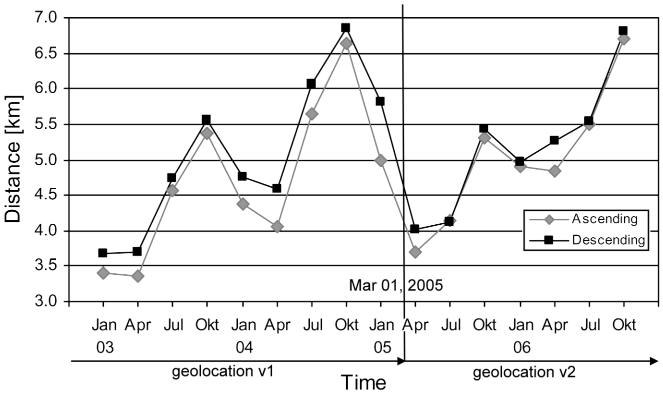

Fig. 8. Changes of repositioning with time between JAXA and IUP geolocation of Channel 89 GHz B-scan H-pol.

C. Numerical Analysis of Viewing Angles

The results obtained from the geolocation optimization for the viewing angles, i.e. nadir angle and scan angle, are shown in Table II. In a first geolocation optimization run, the viewing angles are varied in steps of 0.01° [7]. In a second run, the step size is reduced to 0.002°, which also reduces the standard deviation of the viewing angles. The nadir angle has an average standard deviation of 0.0065° (≈ 224 m) for step size 0.01°, which reduces to 0.0051° (≈ 177 m) for step size 0.002°. The scan angle has an average standard deviation of 0.0081° (≈ 118 m) for step size 0.01°, which reduces to 0.0050° (≈ 73 m) for step size 0.002°. Therefore, for further analysis the results obtained with step size 0.002° will be used.

Variations of the viewing angles of 0.01° correspond to variations on the Earth's surface of 342 m for nadir angle, and 145 m for scan angle. This conversion from degrees of the viewing angles to meters on ground also applies to the standard deviation, which is calculated for the data set of the 16 days.

The values for the optimal nadir angle range from 47.082° to 47.664° with standard deviations between 0.0046° (≈ 156 m) and 0.0063° (≈ 217 m). The values for the optimal scan angle range from 74.848° to 75.410° with standard deviations between 0.0026° (≈ 37 m) and 0.0070° (≈ 101 m).

We define as optimal viewing angles the averaged viewing angles of the 16 selected days from January 2003 to October 2006. Figure 9 illustrates the time series, their mean and their standard deviation for the 89 GHz B-scan data. Similar time series for all other frequencies are given in [7]. The visual analysis does not reveal a time trend in the data. However, there are some quasi-periodic structures in the time series, with minimum values frequently falling into the month of January. This might indicate a remaining error in the geolocation procedure. As the standard deviations correspond to few hundred meters on ground only (Table II), a further analysis of the problem is considered not necessary here.

TABLE II
OPTIMAL VIEWING ANGLES AT ALL AMSR-E FREQUENCIES (STEP SIZE = 0.002°), IN BRACKETS: STANDARD DEVIATION IN DEGREES CONVERTED TO METERS ON GROUND

Channel	Nadir Angle [°]	Scan Angle [°]
6 GHz	47.664 ± 0.0053 (± 183 m)	74.848 ± 0.0034 (± 49 m)
10 GHz	47.638 ± 0.0046 (± 156 m)	74.930 ± 0.0052 (± 75 m)
18 GHz	47.580 ± 0.0047 (± 160 m)	74.936 ± 0.0064 (± 93 m)
23 GHz	47.572 ± 0.0056 (± 192 m)	74.928 ± 0.0058 (± 84 m)
36 GHz	47.586 ± 0.0050 (± 170 m)	74.952 ± 0.0070 (± 101 m)
89 GHz A	47.574 ± 0.0048 (± 163 m)	75.142 ± 0.0026 (± 37 m)
89 GHz B	47.082 ± 0.0063 (± 217 m)	75.410 ± 0.0048 (± 70 m)
Mean	± 0.0052 (± 177 m)	± 0.0050 (± 73 m)

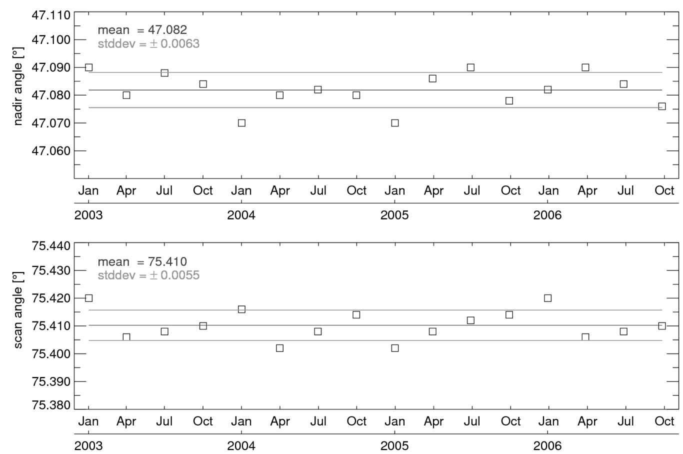

Fig. 9. Optimized viewing angles (top: nadir angle, bottom: scan angle) of Channel 89 GHz B-scan H-pol. from Jan 2003 to Oct 2006.

D. Comparison: IUP versus RSS geolocation

In September 2005, Wentz from Remote Sensing Systems (RSS) presented a geolocation analysis in which a similar approach to optimize the geolocation is used [6]. Table III shows the comparison of optimal viewing angles for all AMSR-E frequencies between the results of IUP and RSS. For easier interpretation, the numerical values are shown as diagrams in Figure 10. The values for the optimal viewing angles are in good agreement. The highest differences between RSS and IUP are 0.016° for the nadir angle (at 36 GHz) and −0.020° for the scan angle (at 23 GHz). The RMS of the differences are 0.008° (≈ 283 m) for the nadir angle and 0.013° (≈ 191 m) for the scan angle. In general, the IUP geolocation confirms the RSS geolocation with small improvements.

IV. SUMMARY AND CONCLUSION

The work presented in this paper allows to locate the observations of AMSR-E much better compared to the geolocation of the original Level 1 data. The averaged repositioning between JAXA and our geolocation ranges between 3.5 km and 7 km.

Looking at the projected brightness temperatures of the AMSR-E data reveals a very good geolocation: Footprints that correspond to water are indeed on water and the ones

TABLE III
COMPARISON OF OPTIMAL VIEWING ANGLES AT ALL AMSR-E FREQUENCIES, IUP VERSUS RSS

Channel	Nadir Angle [°] IUP	RSS	IUP − RSS	
6 GHz	47.664	47.67	−0.006	(≈ −205 m)
10 GHz	47.638	47.64	−0.002	(≈ −68 m)
18 GHz	47.580	47.57	0.010	(≈ 342 m)
23 GHz	47.572	47.57	0.002	(≈ 68 m)
36 GHz	47.586	47.57	0.016	(≈ 547 m)
89 GHz A	47.574	47.57	0.004	(≈ 137 m)
89 GHz B	47.082	47.09	−0.008	(≈ −274 m)
RMS			0.008	(≈ 283 m)

Channel	Scan Angle [°] IUP	RSS	IUP − RSS	
6 GHz	74.848	74.838	0.010	(≈ 145 m)
10 GHz	74.930	74.948	−0.018	(≈ −261 m)
18 GHz	74.936	74.948	−0.012	(≈ −174 m)
23 GHz	74.928	74.948	−0.020	(≈ −290 m)
36 GHz	74.952	74.948	0.004	(≈ 58 m)
89 GHz A	75.142	75.148	−0.006	(≈ −87 m)
89 GHz B	75.410	75.424	−0.014	(≈ −203 m)
RMS			0.013	(≈ 191 m)

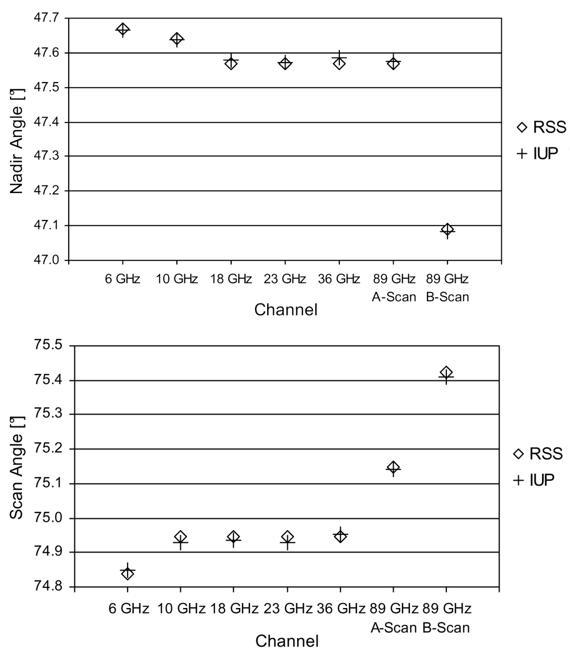

Fig. 10. Comparison (IUP versus RSS) of optimal viewing angles at all AMSR-E channels

referring to land are indeed on land (Figure 3). The visual analysis of the difference plots (ascending minus descending) before and after adjusting the geolocation shows that there are almost no coastline differences due to geolocation after the correction (Figure 4). The mean difference of ascending minus descending swaths has been reduced from values between 9 K and 16 K per pixel (higher differences at higher frequency channels, Table I) by about 50% to values between 5 K and 8 K per pixel. The remaining differences can be attributed to different surface temperatures and different atmospheric conditions at the acquisition time (the latter especially affects the 89 GHz channels, see Figure 4 bottom for examples). The residual geolocation error ranges from 245 m for the 89 GHz channels (5% of the footprint size) to 1425 m for the 6 GHz channel (2% of the footprint size).

The resulting optimal viewing angles are given in Table II. The time series of these optimal parameters does show no trend, it is randomly distributed with an overall mean standard deviation of 0.005° (averaged over all AMSR-E channels), which corresponds to a distance on the Earth's surface of 170 m for the nadir angle and 70 m for the scan angle.

The comparison with the parameters from a similar study by Wentz [6] shows good agreement. The highest difference for the nadir angle is 0.016° (≈ 547 m), for the scan angle it is 0.02° (≈ 290 m). These differences are significant because they are over three times the standard deviation of our geolocation.

In this study we focussed the geolocation analysis on the viewing angles. The small remaining errors of few hundred meters indicate that these angles constitute the main contribution to the current JAXA geolocation. Further sources for the geolocation error, e.g. the time offsets between the spacecraft ephemeris time and the time associated with the sampled AMSR-E data, may only have a minor influence, as we achieve very accurate results by our optimized viewing angles.

ACKNOWLEDGMENT

This study was supported by EU project DAMOCLES (Developing Arctic Modeling and Observing Capabilities for Long-term Environmental Studies) and DFG grant He 1746/10-3.

REFERENCES

[1] K. Imaoka, Y. Fujimoto, M. Kachi, T. Takeshima, K. Shiomi, H. Mikai, T. Mutoh, M. Yoshikawa, A. Shibata: *Post-launch calibration and data evaluation of AMSR-E*. In Proc. IGARSS, vol. 1, pp. 666-668, 2003.

[2] JAXA: *AMSR-E Level 1 Product Format Description.* Technical Report, 2005, URL www.eoc.jaxa.jp/amsr-e/amsr-e_format_l1_e.pdf.

[3] T. Takeshima (JAXA): *Geo-location Errors*. Presentation during Joint AMSR Science Team Meeting, Honolulu, Hawaii, 2005, URL www.ghcc.msfc.nasa.gov/AMSR/meetings2005/takeshima_geolocation.pdf.

[4] T. Kawanishi, T. Sezai, Y. Ito, K. Imaoka, T. Takeshima, Y. Ishido, A. Shibata, M. Miura, H. Inahata, R.W. Spencer: *The Advanced Microwave Scanning Radiometer for the Earth Observing System (AMSR-E), NASDA's Contribution to the EOS for Global Energy and Water Cycle Studies*. IEEE Transactions on Geoscience and Remote Sensing, vol. 41, pp. 184-194, 2003.

[5] L. Meyer-Lerbes, *IUP AMSR-E Reprojection*. Internal Document, Institute of Environmental Physics, University Bremen, 2006.

[6] F. Wentz, P. Ashcroft, M. Brewer: *AMSR-E geolocation analysis.* Presentation during Joint AMSR Science Team Meeting, Honolulu, Hawaii, 2005, URL http://www.ghcc.msfc.nasa.gov/AMSR/meetings2005/wentz_calibration_hawaii_2005.pdf.

[7] H. Wiebe: *Validation of the ARTIST Sea Ice (ASI) Concentration Algorithm and Geolocation of the Microwave Radiometer AMSR-E data*, Master Thesis, University Bremen, 2007.

[8] R.E. Wolfe, M. Nishihama, A.J. Fleig, J.A. Kuyper, D.P. Roy, J.C. Storey, F.S. Patt: *Achieving sub-pixel geolocation accuracy in support of MODIS land science*, Remote Sensing of the Environment, vol. 83(1-2), pp. 31-49, 2002.

[9] R.E. Wolfe, V.V. Salomonson: *MODIS geolocation approach, results and the future*, Advances in Techniques for Analysis of Remotely Sensed Data, pp. 424-427, IEEE Workshop on 27.-28. Oct, 2003.